ELSEVIER

Biochimica et Biophysica Acta 1510 (2001) 219–230

BIOCHIMICA ET BIOPHYSICA ACTA
BBA

www.elsevier.com/locate/bba

The effect of ethanol on the phase transition temperature and the phase structure of monounsaturated phosphatidylcholines

Thomas J. McIntosh [a], Hainan Lin [b], Shusen Li [b], Ching-hsien Huang [b,*]

[a] *Department of Cell Biology, Duke University Medical Center, Durham, NC 27710, USA*
[b] *Department of Biochemistry and Molecular Genetics, University of Virginia School of Medicine, P.O. Box 800733, Charlottesville, VA 22908, USA*

Received 3 August 2000; received in revised form 17 October 2000; accepted 17 October 2000

Abstract

Previous studies from our laboratories have delineated the relationship between the acyl chain asymmetry of mixed-chain phosphatidylcholines, C(X):C(Y)PC, and the effect of ethanol concentration, [EtOH], on the main phase transition temperature, T_m, and the phase structure of the lipid bilayer composed of C(X):C(Y)PC using differential scanning calorimetry and X-ray diffraction techniques [Huang and McIntosh, Biophys. J. 72 (1997) 2702–2709]. In the present work, we have extended these studies to characterize the effect of [EtOH] on the T_m and the phase structure of the lipid bilayer composed of *sn*-1 saturated/*sn*-2 monounsaturated phosphatidylcholines with various positions of the *cis* double bond. Specifically, five positional isomers of 1-eicosanoyl-2-eicosenoyl-*sn*-glycero-3-phosphocholines, C(20):C(20:1Δ^n)PC with $n=5$, 8, 11, 13 and 17, were synthesized and studied. For C(20):C(20:1Δ^n)PC with $n=5$ and 8, results from the calorimetric experiments showed that in response to various concentrations of ethanol, the change in T_m of the lipid bilayer composed of monounsaturated lipids was characterized by a sigmoidal or biphasic profile in the plot of T_m versus [EtOH]. In contrast, a continuous depression of the T_m by ethanol was observed calorimetrically for C(20):C(20:1Δ^n)PC with $n \geq 11$. The X-ray diffraction experiments further demonstrated that C(20):C(20:1Δ^5)PC and C(20):C(20:1Δ^8)PC can undergo the ethanol-induced gel-to-fully interdigitated phase transition at $T < T_m$. Such a transition, however, was not observed for C(20):C(20:1Δ^{13})PC even at a very high ethanol concentration of 100 mg/ml. These distinct different effects of [EtOH] on the phase transition temperature and the phase structure can be attributed to various positions of the *cis* double bond in these monounsaturated phosphatidylcholines. And the different effects of ethanol can, in fact, be explained based on the molecular structures of these monounsaturated lipids packed in the gel-state bilayer as generated by molecular mechanics simulations. To the best of our knowledge, this is the first time that the ethanol-induced fully interdigitated bilayers are observed at $T < T_m$ for unsaturated phospholipids with well defined double bond positions in their *sn*-2 acyl chains.

Keywords: Differential scanning calorimetry; Interdigitation; Molecular mechanics simulation; Monounsaturated lipid; X-ray diffraction

Abbreviations: C(X):C(Y)PC, saturated diacyl phosphatidylcholine with X and Y carbons in the *sn*-1 and *sn*-2 acyl chains, respectively; C(20):C(20:1Δ^n)PC, 1-eicosanoyl-2-eicosenoyl-*sn*-glycero-3-phosphocholine with the single *cis* double bond at the *n*th carbon atom from the carbonyl end (Δ^n); DSC, differential scanning calorimetry; [EtOH], ethanol concentration in mg/ml; $L_{\beta'}$, tilted gel-phase; $L_{\beta I}$, fully interdigitated gel-phase; PC, phosphatidylcholine; T_m, phase transition temperature associated with the gel-to-liquid crystalline phase transition

* Corresponding author. Fax: +1-804-924-5069; E-mail: ch9t@virginia.edu

0005-2736/01/$ – see front matter
PII: S0005-2736(00)00352-7

1. Introduction

The biphasic effect of ethanol on the main phase transition temperature, T_m, of lipid bilayers composed of saturated identical-chain phosphatidylcholines (PC), or C(X):C(X)PC, has been well documented [1]. For instance, the T_m value of C(16):C(16)PC constituting lipid bilayers in the aqueous dispersion is 41.6°C in the absence of ethanol. This T_m value is shifted in a down-and-up manner when a series of ethanol solutions is added successively into the aqueous lipid dispersion. Specifically, as the ethanol concentration (in mg/ml), [EtOH], in the aqueous dispersion is increased initially, the T_m value of C(16):C(16)PC is observed to decrease almost linearly, reaching a nadir of 39.4°C at an ethanol concentration of $\sim$50 mg/ml. Thereafter, the T_m value of C(16):C(16)PC increases as the [EtOH] is increased up to 120 mg/ml, resulting in a V-shaped T_m profile in the plot of T_m versus [EtOH]. The ethanol concentration that corresponds to the inflection point in the V-shaped T_m profile is called the 'threshold concentration'. This threshold concentration, abbreviated as $[EtOH]_{TC}$, is found to decrease curvilinearly with increasing chain length for a homologous series of saturated identical-chain C(X):C(X)PC ranging from C(14):C(14)PC to C(21):C(21)PC [1]. In fact, in the plot of $[EtOH]_{TC}$ versus the T_m exhibited by C(X):C(X)PC in the absence of ethanol, a straight line with a negative slope can be detected for this homologous series of saturated identical-chain C(X):C(X)PC. For saturated mixed-chain C(X):C(Y)PC (saturated diacyl PC with X and Y carbons in the *sn*-1 and *sn*-2 acyl chains, respectively) with $\Delta C < 4.2$ C–C bond lengths, the T_m profile in the plot of T_m versus [EtOH] is also V-shaped [2]. Here, the structural parameter ΔC refers to the effective chain length difference between the two acyl chains of lipid in the gel-state bilayer. For instance, the ΔC values for the two positional isomers of C(15):C(17)PC and C(17):C(15)PC are 0.5 and 3.5 C–C bond lengths, respectively. Classical V-shaped T_m profiles are observed for C(15):C(17)PC and C(17):C(15)PC with $[EtOH]_{TC}$ values being 50 and 73 mg/ml, respectively [2]. In the absence of ethanol, the C(15):C(17)PC and C(17):C(15)PC bilayers exhibit T_m values of 41.7 and 37.7°C, respectively. Hence, for these two positional isomers with mixed acyl chains, the one with a higher T_m value exhibits a smaller $[EtOH]_{TC}$ value in response to ethanol. Most importantly, it was shown by X-ray diffraction that, at 20°C, C(16):C(16)PC, C(15):C(17)PC and C(17):C(15)PC share a common packing motif, when the equilibrium concentration of the incubating ethanol is 120 mg/ml, which is considerably greater than $[EtOH]_{TC}$ [3,4]. In this packing motif, the two acyl chains of each lipid molecule extend across the whole width of the hydrocarbon core with their terminal methyl groups being exposed to the ethanol–water medium. The lipid bilayer that exhibits such a fully interdigitated packing motif, at $T < T_m$, is called the $L_{\beta I}$-phase (fully interdigitated gel-phase) bilayer. The X-ray diffraction data also show that these saturated lipids, C(16):C(16)PC, C(15):C(17)PC and C(17):C(15)PC, form the normal $L_{\beta'}$-phase (tilted gel-phase) lipid bilayer at 20°C in the absence of ethanol [3,4]. The V-shaped T_m profiles exhibited by these saturated lipids in response to various concentrations of ethanol can thus be explained by the $L_{\beta'} \rightarrow L_{\beta I}$ isothermal phase transition, at $T < T_m$, induced by concentrations of ethanol above the threshold concentration [3].

Although the biphasic effect of ethanol on the T_m of the lipid bilayer composed of PC has been studied exhaustively, the lipid bilayers employed in these studies are prepared exclusively from either saturated identical-chain C(X):C(X)PC or saturated mixed-chain C(X):C(Y)PC. It is well known, however, that membrane PCs isolated from animal cells are commonly mixed-chain unsaturated PC, in which a saturated long-chain fatty acid and an unsaturated long-chain fatty acid with *cis* C–C double bonds are esterified at C-1 and C-2 of the glycerol backbone, respectively [5]. Moreover, the number and position of *cis* double bonds (Δ) in the *sn*-2 acyl chain of membrane PC may vary considerably. It is thus of biological relevance to study the effects of ethanol on the T_m of lipid bilayers comprised of unsaturated mixed-chain PC with various numbers and positions of Δ-bonds in the *sn*-2 acyl chain. As a first step to investigate the effects of ethanol on the T_m of unsaturated mixed-chain PC, a series of five double-bond positional isomers of monounsaturated mixed-chain PC was first synthesized as described in this communication. Specifically, 1-eicosanoyl-2-eicosenoyl-*sn*-glycero-3-phosphocholines [C(20):C(20:1Δ^n)PC]

with $n = 5$, 8, 11, 13 and 17 were chosen, where the superscript n of Δ^n refers to the Δ-bond position at the nth carbon atom from the carbonyl end along the *sn*-2 acyl chain. Subsequently, the phase transition behavior of this series of C(20):C(20:1Δ^n)PC in the presence of various concentrations of ethanol was studied by differential scanning calorimetry (DSC). In parallel, the possible ethanol-induced $L_{\beta'} \rightarrow L_{\beta I}$ isothermal phase transition, at $T < T_m$, was also investigated by X-ray diffraction techniques. Interestingly, the biphasic effect of ethanol on T_m was observed calorimetrically for C(20):C(20:1Δ^n)PC with $\Delta^n = 5$ and 8. Moreover, X-ray diffraction results showed that the lipid bilayers prepared individually from these two unsaturated lipids, C(20):C(20:1Δ^n)PC with $\Delta^n = 5$ and 8, can transform into the fully interdigitated ($L_{\beta I}$) gel-state bilayers at $[EtOH] > [EtOH]_{TC}$. In this communication, the ethanol-induced isothermal $L_{\beta'} \rightarrow L_{\beta I}$ phase transition is thus clearly demonstrated, for the first time, to take place in the lipid bilayer that contains biologically relevant mixed-chain phospholipids.

2. Materials and methods

2.1. Semi-synthesis of monoenoic mixed-chain PC with 20 carbons in each acyl chain or 1-eicosanoyl-2-eicosenyl-sn-glycero-3-phosphocholines [C(20):C(20:1Δ^n)PC]

All chemicals used in the semi-synthesis of C(20):C(20:1Δ^n)PC were of reagent grade, and all solvents were of spectroscopic grade. The C(20)-lysophosphatidylcholines were purchased from Avanti Polar Lipids (Alabaster, AL, USA). With the exception of *cis*-17-eicosenoic acid, all other monoenoic C(20)-fatty acids were obtained from Sigma (St. Louis, MO, USA). *Cis*-17-eicosenoic acid was de novo synthesized in the laboratory using the method published recently [6]. Each of the following five positional isomers of the monoenoic mixed-chain PC was semi-synthesized, in the presence of the catalyst 4-pyrrolidinopyridine, from C(20)-lysophosphatidylcholine and the corresponding monoenoic C(20)-fatty acid at room temperatures according to the established procedure published previously [7]: C(20):C(20:1Δ^n)PC, where $n = 5$, 8, 11, 13 and 17. The lipids were then purified by column chromatography using Silica Gel 60 (mash size, 230–400) (Sigma), and they were judged to be $\sim$98% isomerically pure [7]. Prior to use, the purified lipids were lyophilized and the resulting lipid powder was stored under an N_2 atmosphere at -20°C.

2.2. High-resolution DSC

Prior to DSC experiments, the aqueous dispersion of purified mixed-chain lipid with a defined concentration was prepared by dispersing the pre-weighted lipid power in a known volume of aqueous solution containing 50 mM NaCl, 1 mM EDTA, 5 mM phosphate buffer, pH 7.4. The lipid concentration, usually $\sim$4 mg/ml, was also checked by inorganic phosphate determination. The aqueous lipid sample (2 ml) was sealed under a N_2 atmosphere and heated to a temperature of $\sim$15°C above the T_m of the lipid. Subsequently, the lipid sample was subjected to ultrasonic irradiation in an ultrasonic water bath at the elevated temperature for up to 30 min. Aliquots of absolute ethanol (10–250 μl) were added to the lipid solution to give the final desired [EtOH]. The lipid/ethanol sample was resealed followed by vortexing for several minutes at the room temperature, and then equilibrated at 4°C for a minimal of 4 h prior to injection into the sample cell of the differential scanning calorimeter.

The thermotropic phase behavior of the lipid/ethanol samples was studied using a high-resolution MC-2 differential scanning calorimeter (Microcal, Northampton, MA, USA), as previously described [7]. A nominal heating rate of 15°C/h was used for all samples and, for each sample, the reference cell of the calorimeter was filled with buffer solution containing the same ethanol concentration as that of the lipid/ethanol sample [2,4]. In general, each lipid/ethanol sample was run successively four times over a temperature range of 30°C ($T_m \pm 15$°C) using the upscan mode. In this mode, DSC measured continuously the excess heat capacity as a function of ascending temperature. The four DSC heating curves recorded for each lipid/ethanol sample were analyzed using the software provided by Microcal. Specifically, the main phase transition temperature, T_m, exhibited by the lipid/ethanol sample was taken as the temperature at which the excess heat capacity reached a

maximum in the DSC heating curve. In these DSC experiments, the values of T_m determined from the second, third and fourth DSC heating curves were virtually identical, with a difference among them being well within ±0.05°C. The T_m value determined from the second DSC heating scan was thus taken uniformly in this communication as the experimental T_m value.

2.3. X-ray diffraction

For X-ray diffraction analysis, multiwalled vesicles were prepared by adding dry lipid to excess buffer (50 mM NaCl, 1 mM EDTA, 5 mM phosphate buffer, pH 7.0) or the same buffer containing specified concentrations of EtOH. The suspensions were heated to 50°C three times for 30 min, extensively vortexed, pelleted with a bench centrifuge, sealed in quartz glass X-ray capillary tubes, and mounted in a point collimation X-ray camera. X-ray diffraction patterns were recorded on stacks of Kodak DEF X-ray film which were densitometered with a Joyce-Loebl microdensitometer. After background subtraction, integrated intensities, $I(h)$, were obtained for each order h by measuring the area under each diffraction peak as described previously [8,9]. For these patterns from unoriented suspensions the structure amplitudes $F(h)$ were set equal to $\{h2I(h)\}^{1/2}$. Electron density profiles, $\rho(x)$, on a relative electron density scale were calculated from:

$$\rho(x) = (2/d)\sum \exp\{i\phi(h)\}F(h)\cos(2\pi xh/d) \qquad (1)$$

where x is the distance from the center of the bilayer, d is the lamellar repeat period, $\phi(h)$ is the phase angle for order h, and the sum is over h. As described elsewhere, phase angles were determined by comparison with previous diffraction analyses [9,10].

3. Results

3.1. The ethanol effect on the T_m of aqueous dispersions of 1-eicosanoyl-2-eicosenoyl-sn-glycero-3-phosphocholines

Fig. 1 shows a series of DSC heating thermograms for the aqueous dispersions of C(20):C(20:1Δ^8)PC containing different [EtOH]. The T_m value obtained with lamellar C(20):C(20:1Δ^8)PC at different [EtOH] is shown next to each DSC curve in Fig. 1. It is evident that at relatively low [EtOH], ethanol causes a downward shift in the phase transition curve, whereas an upward shift is seen at higher [EtOH]. In the plot of T_m versus [EtOH], a V-shaped T_m profile with a distinct inflection point is observed for C(20):C(20:1Δ^8)PC as shown in the lower inset of Fig. 1. The ethanol concentration of 60 mg/ml at the T_m-inflection point is by definition the value of $[EtOH]_{TC}$. For comparison, we have also studied the biphasic effect of ethanol on the T_m of saturated mixed-chain C(20):C(19)PC. We have chosen C(20):C(19)PC based on the fact that the *sn*-2 acyl chain length of C(20):C(19)PC in the crystalline bilayer is virtually identical to that of C(20):C(20:1Δ^8)PC. In the absence of ethanol, the T_m value obtained calorimetrically with C(20):C(19)PC is 61.4°C. In the presence of various concentrations of ethanol, the apparent T_m values for C(20):C(19)PC are plotted against [EtOH] in the upper inset of Fig. 1. Clearly, the resulting T_m curve is biphasic with the inflection point occurring at $[EtOH]_{TC}$ of 15 mg/ml. This $[EtOH]_{TC}$ value is significantly smaller than that of 60 mg/ml observed for C(20):C(20:1Δ^8)PC.

Fig. 2 shows the results of a second series of DSC experiments, in which the addition of ethanol is observed to cause a shift in the phase transition curve for the aqueous dispersions of C(20):C(20:1Δ^{13})PC. Unlike C(20):C(20:1Δ^8)PC, the phase transition curve of C(20):C(20:1Δ^{13})PC shifts continuously toward a lower temperature as [EtOH] increases from one DSC curve to another. In the plot of T_m versus [EtOH], the apparent T_m values associated with these DSC curves fall on a nearly straight line with a negative slope (the lower inset, Fig. 2). Similar T_m profiles with negative slopes have also been observed previously for saturated highly asymmetric PC such as C(12):C(20)PC and C(18):C(14)PC [2,4].

In an attempt to examine fully how variations in the position of a single *cis* double bond affect the response of monounsaturated PC to ethanol, we have, in addition to C(20):C(20:1Δ^8)PC and C(20):C(20:1Δ^{13})PC, further studied the effects of ethanol on the T_m of C(20):C(20:1Δ^n)PC with $n=5$, 11 and 17. In the absence of ethanol, the T_m values of C(20):C(20:1Δ^n)PC with $n=5$, 8, 11, 13

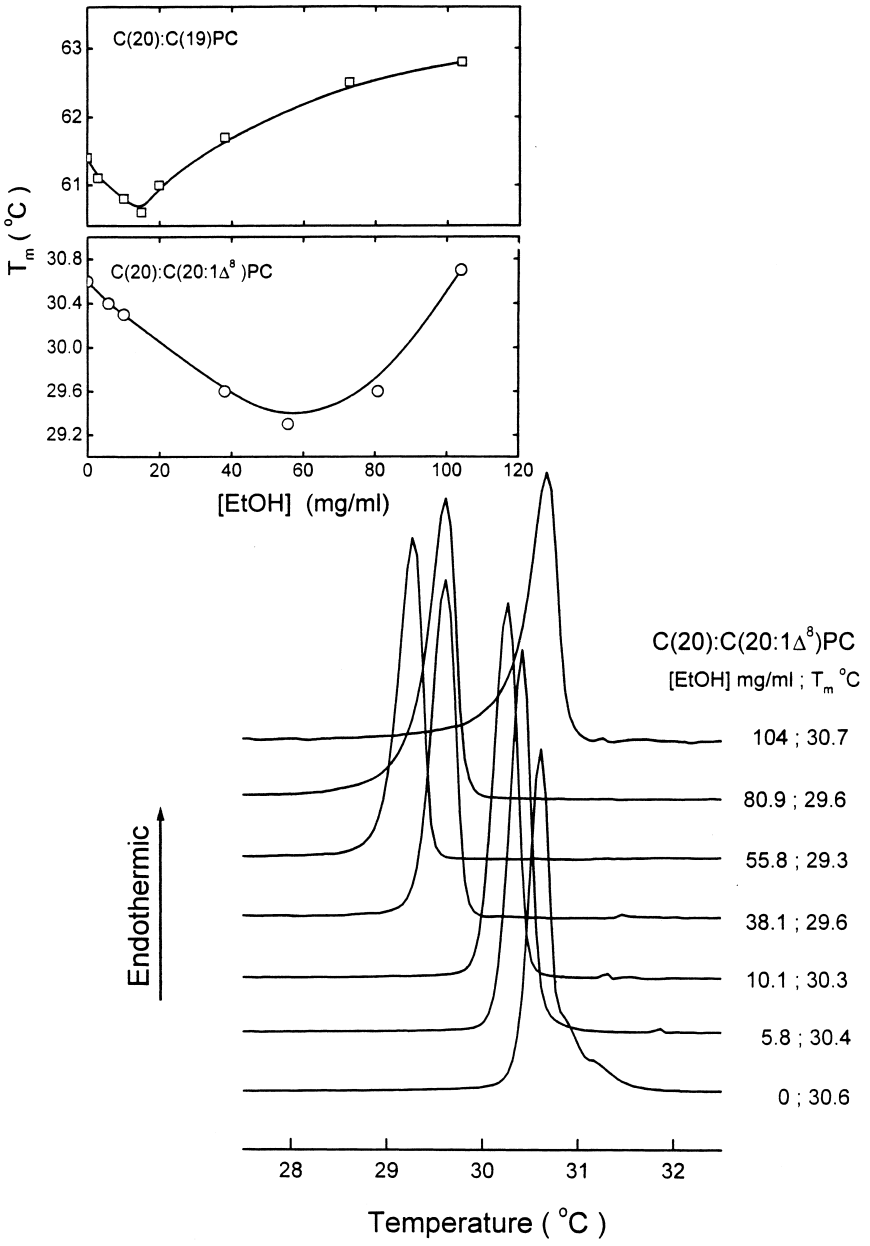

Fig. 1. The effect of ethanol concentration, [EtOH], on the phase transition behavior of the aqueous dispersion of C(20):C(20:1Δ^8)PC. The representative DSC curves are the second DSC heating curves, and the [EtOH] and T_m values are indicated on the right side of each corresponding DSC curve. Scan rate: 15°C/h. The T_m value of unsaturated C(20):C(20:1Δ^8)PC is also plotted against [EtOH] as shown in the lower inset giving rise to a biphasic T_m profile. For comparison, the T_m value of saturated C(20):C(19)PC is also plotted against [EtOH] as shown in the upper inset.

and 17 are 44.9, 30.6, 19.4, 22.1 and 49.7°C, respectively, which are in good agreement with the literature values [11]. And all these values are plotted against the position of Δ^n in the inset of Fig. 3, giving rise to an inverted bell-shaped curve with the minimum T_m occurring at $n \cong 11$. We can define a term ΔT_m as the difference between the phase transition temperature of the lipid sample prepared in the presence of a given [EtOH] and the T_m of the aqueous lipid dispersion prepared from the same lipid in the absence of ethanol. With this normalized parameter, ΔT_m, a large number of the phase transition temper-

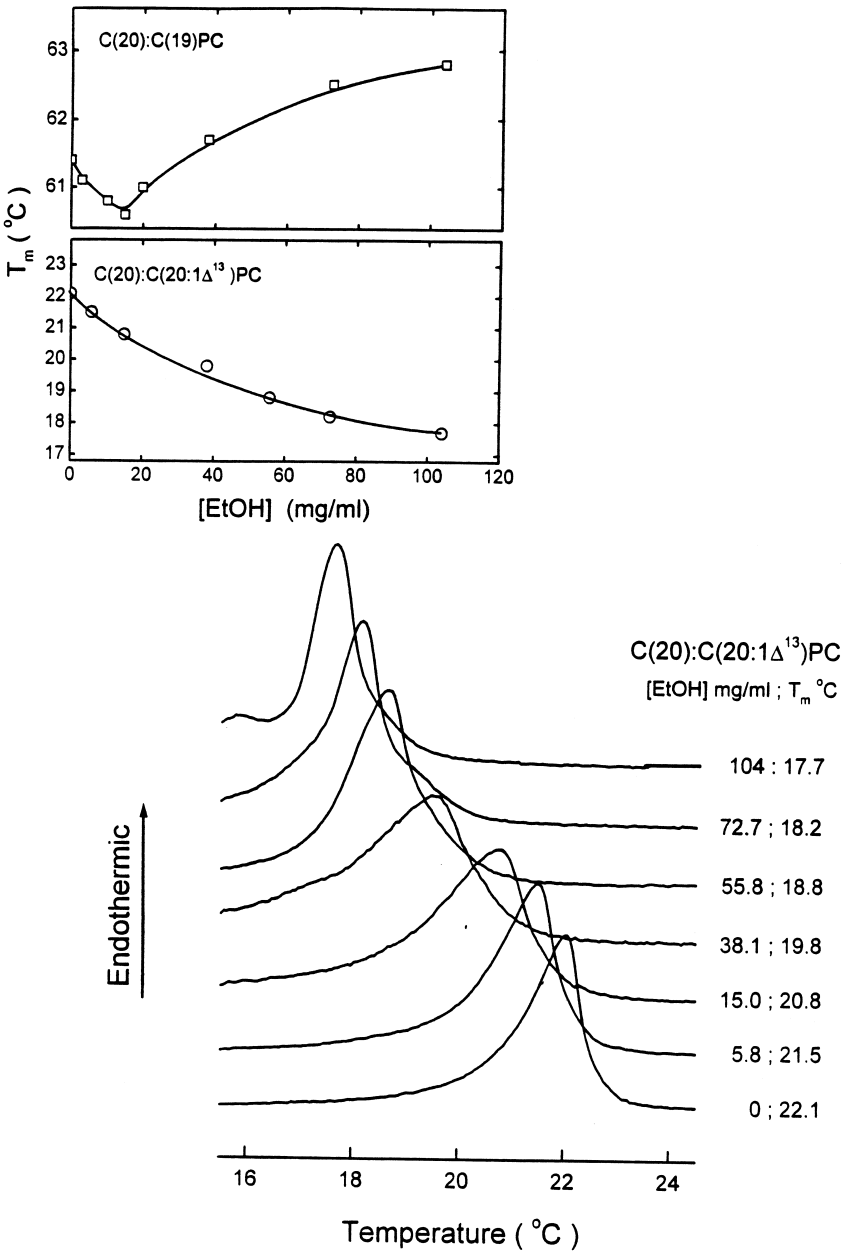

Fig. 2. The effect of ethanol concentration, [EtOH], on the phase transition behavior of C(20):C(20:1Δ^{13})PC. The [EtOH] and T_m values associated with each DSC curve are indicated on the right-hand side of the corresponding DSC curve. The upper and lower insets show the plots of T_m versus [EtOH] for C(20):C(19)PC and C(20):C(20:1Δ^{13})PC, respectively.

atures exhibited by C(20):C(20:1Δ^n)PC with $n=5$, 8, 11, 13 and 17 in the presence of various concentrations of ethanol can all be compared simultaneously in a single plot. This plot of ΔT_m against [EtOH] for all five positional isomers of C(20):C(20:1Δ^n)PC is depicted in Fig. 3. One distinct feature is immediately evident from this plot, viz. the effect of ethanol on ΔT_m depends critically on the position of the *cis* double bond (Δ^n) in the *sn*-2 acyl chain. For instance, a biphasic effect of ethanol on ΔT_m is observed for C(20):C(20:1Δ^8)PC with a $[EtOH]_{TC}$ value of 60 mg/ml. This V-shaped ΔT_m profile suggests that C(20):C(20:1Δ^8)PC are packed, at $T < T_m$, in the L_β-phase bilayer at [EtOH] <60 mg/ml and that

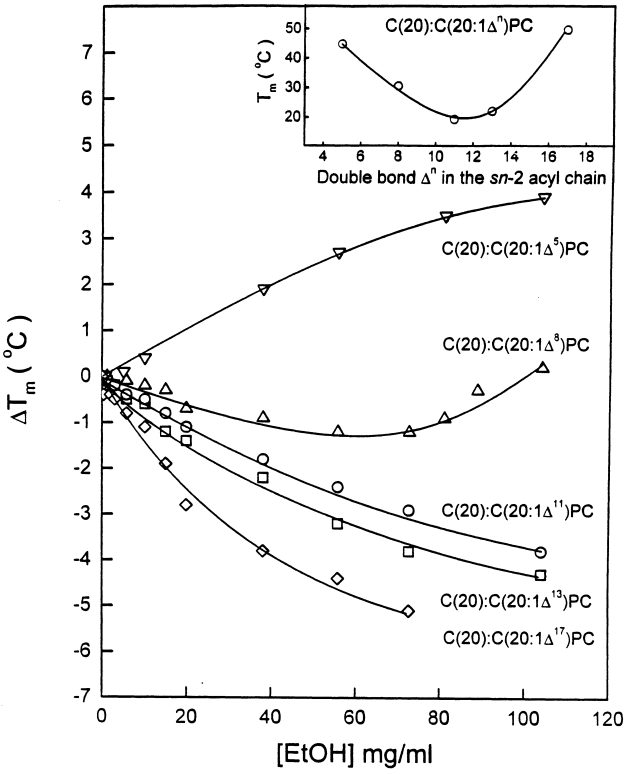

Fig. 3. The plot of ΔT_m versus [EtOH] for C(20):C(20:1Δ^n)PC with $n=5$, 8, 11, 13 and 17. ΔT_m denotes the difference between the phase transition temperature of the lipid sample prepared in presence of a given [EtOH] and the T_m exhibited by the same lipid in the absence of ethanol. The T_m values of lipids in this series of C(20):C(20:1Δ^n)PC obtained in the absence of ethanol are also plotted against the position of the double bond (Δ^n) as shown in the inset.

the L_β-phase bilayer of C(20):C(20:1Δ^8)PC transforms isothermally into the $L_{\beta I}$-phase bilayer at [EtOH] > 60 mg/ml. As the *cis* double bond migrates toward the hydrocarbon/H_2O interface as exemplified by C(20):C(20:1Δ^5)PC, the ΔT_m profile shown in Fig. 3 is no longer V-shaped. Instead, a sigmoid-shaped profile with a positive slope is observed. Such a sigmoidal ΔT_m profile suggests that for C(20):C(20:1Δ^5)PC the isothermal $L_\beta \rightarrow L_{\beta I}$ phase transition can be induced by a minimum of 5 mg/ml of ethanol, which is significantly lower than the $[EtOH]_{TC}$ value of 60 mg/ml observed for C(20):C(20:1Δ^8)PC. Interestingly, as the *cis* double bond moves stepwise from the Δ^8-position toward the methyl end, the ΔT_m profiles exhibited by C(20):C(20:1Δ^{11})PC, C(20):C(20:1Δ^{13})PC and C(20):C(20:1Δ^{17})PC are each characterized by a nearly straight line with a negative slope as shown in Fig. 3. Since no inflection points in the ΔT_m profiles are detected for C(20):C(20:1Δ^{11})PC, C(20):C(20:1Δ^{13})PC and C(20):C(20:1Δ^{17})PC in the plot of ΔT_m versus [EtOH], the ΔT_m value observed for each of the three positional isomers at a given [EtOH] represents the magnitude of the T_m depression induced by ethanol at that specific ethanol concentration.

3.2. X-ray diffraction

For all lipid dispersions, each X-ray diffraction pattern contained a series of low-angle reflections that indexed as orders of a single lamellar repeat period, along with one or two wide-angle reflections. The lamellar repeat period and the wide-angle spacing varied, depending both on the lipid and the amount of EtOH in the buffer.

For both C(20):C(20:1Δ^5)PC and C(20):C(20:1Δ^8)PC the repeat period was 86 Å and the wide-angle region contained a rather broad reflection centered at 4.21 Å. However, the presence of EtOH changed both the low- and wide-angle spacings. In the case of C(20):C(20:1Δ^5)PC the presence of 20, 40 or 100 mg/ml gave a pattern containing several orders of 56 Å lamellar repeat period and a very sharp 4.10 Å wide-angle reflection. In the case of C(20):C(20:1Δ^8)PC, the presence of 80 mg/ml EtOH produced no change in the diffraction pattern, whereas the presence of 120 mg/ml EtOH produced a pattern with a lamellar spacing of 57 Å and a very sharp wide-angle spacing of 4.10 Å. For C(20):C(20:1Δ^{13})PC, the X-ray patterns were the same in the presence and absence of 100 mg/ml EtOH and consisted of a lamellar repeat period of 71 Å and two wide-angle spacing, a sharp reflection at 4.31 Å and a broad reflection at 4.17 Å.

Electron density profiles were calculated by using the same phase angles as previously obtained for saturated PCs in the presence and absence of EtOH [8,9]. Representative profiles are shown in Fig. 4. In each profile, the bilayer center is located at the origin, so that the low electron density region in the center of each profile corresponds to the lipid hydrocarbon regions. The high density peaks, located at ±18 Å for both C(20):C(20:1Δ^5)PC and C(20):C(20:1Δ^8)PC and at ±25 Å for C(20):

C(20:1Δ^{13})PC, correspond to the lipid polar head groups. Thus, the bilayer thickness, as measured by the distance between the high density headgroups, is considerably larger for C(20):C(20:1Δ^{13})PC in the presence of 100 mg/ml EtOH compared to either C(20):C(20:1Δ^{5})PC with 20 mg/ml EtOH or C(20):C(20:1Δ^{8})PC with 120 mg/ml EtOH. For C(20):C(20:1Δ^{13})PC in the presence of 100 mg/ml EtOH there is a sharp dip in electron density in the geometric center of the bilayer, whereas for both C(20):C(20:1Δ^{5})PC at 20 mg/ml EtOH and C(20):C(20:1Δ^{8})PC at 120 mg/ml, there is no such trough in the bilayer center. Such central electron density troughs are caused by the localization of the hydrocarbon chain terminal methyl groups in the center of the bilayer [9,12], which is typical of bilayers in the non-interdigitated $L_{\beta'}$ phase. The absence of this central trough, such as seen with both C(20):C(20:1Δ^{5})PC at 20 mg/ml EtOH and C(20):C(20:1Δ^{8})PC at 120 mg/ml (Fig. 4), is typical of bilayers in the fully interdigitated phase ($L_{\beta I}$), where the hydrocarbon chains from apposing monolayers of the bilayer interpenetrate so that the terminal methyl groups are located near the hydrocarbon–water interface [10].

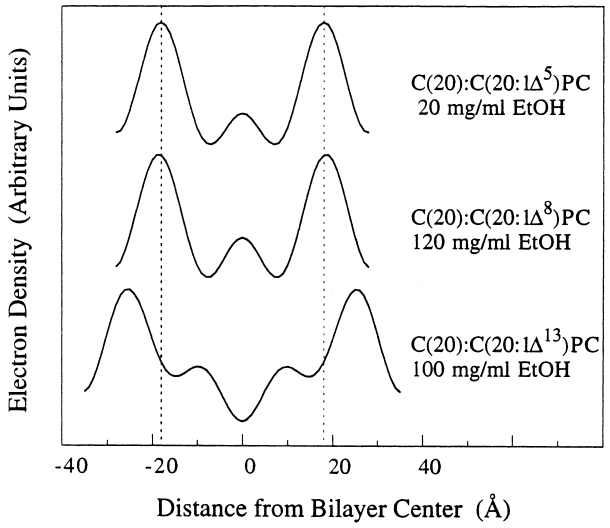

Fig. 4. Electron density profiles for bilayers of C(20):C(20:1Δ^{5})PC in the presence of 20 mg/ml EtOH, C(20):C(20:1Δ^{8})PC with 120 mg/ml EtOH, and C(20):C(20:1Δ^{13})PC with 100 mg/ml EtOH. For each profile the geometric center of the bilayer is located at the origin, and the high density peaks, located at ±18 Å for both C(20):C(20:1Δ^{5})PC and C(20):C(20:1Δ^{8})PC (denoted by the vertical dotted lines) and ±25 Å for C(20):C(20:1Δ^{13})PC, correspond to the lipid polar headgroups.

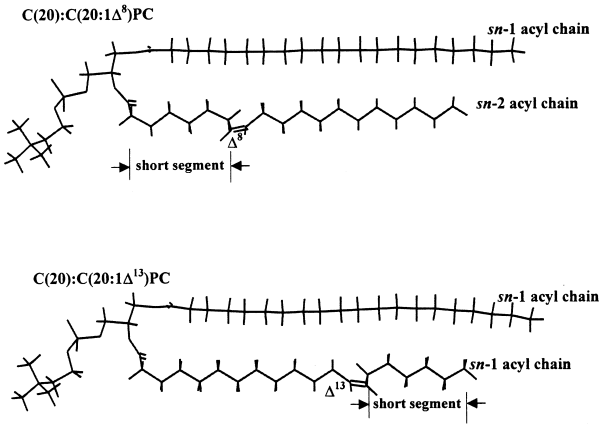

Fig. 5. Molecular graphic representations of the energy-minimized structures of C(20):C(20:1Δ^{8})PC and C(20):C(20:1Δ^{13})PC. It should be noted that the monounsaturated *sn*-2 acyl chain of each lipid molecule adopts a crankshaft-like motif with two unequal chain segments. For C(20):C(20:1Δ^{8})PC, the short chain segment is positioned near the H_2O/hydrocarbon interface. In contrast, the short chain segment is closer to the bilayer center for C(20):C(20:1Δ^{13})PC.

The wide-angle X-ray reflections also indicate that in the presence of EtOH, C(20):C(20:1Δ^{5})PC and C(20):C(20:1Δ^{8})PC, but not C(20):C(20:1Δ^{13})PC, form an interdigitated phase. That is, the single sharp wide-angle reflection at the relatively small spacing of 4.10 Å is typical of PCs in the $L_{\beta I}$ phase, whereas the single broad reflection at 4.21 Å (observed for C(20):C(20:1Δ^{5})PC and C(20):C(20:1Δ^{8})PC in the absence of EtOH) or the doublet of a sharp and broad reflections (observed for C(20):C(20:1Δ^{13})PC in the presence or absence of EtOH) are consistent with tilted hydrocarbon chains, or bilayers in the non-interdigitated $L_{\beta'}$ phase [10].

4. Discussion

We have examined the effect of ethanol on the phase transition temperature (T_m) as well as the phase structure of a series of five positional isomers of monounsaturated C(20):C(20:1Δ^{n})PC by high-resolution DSC and X-ray diffraction techniques. As summarized in Fig. 3, our DSC results show that, in response to ethanol, variations in the normalized

T_m values of C(20):C(20:1Δ^n)PC with $n<11$ differ markedly from those of C(20):C(20:1Δ^n)PC with $n\geq 11$. Specifically, when the *cis* C–C double bond is positioned in the upper segment of the *sn*-2 C_{20}-acyl chain such as C(20):C(20:1Δ^5)PC and C(20):C(20:1Δ^8)PC, the variation in the normalized T_m of these lipids as a function of [EtOH] is characterized by a sigmoidal or biphasic profile. In contrast, over a wide range of [EtOH], a continuous depression of the T_m by ethanol is observed for C(20):C(20:1Δ^n)PC with $n\geq 11$. The results of X-ray diffraction experiments further demonstrate that C(20):C(20:1Δ^5)PC and C(20):C(20:1Δ^8)PC can undergo the ethanol-induced $L_{\beta'}\rightarrow L_{\beta I}$ phase transition, with C(20):C(20:1Δ^5)PC undergoing the transition at lower ethanol concentrations than C(20):C(20:1Δ^8)PC (Fig. 4). However, the $L_{\beta'}\rightarrow L_{\beta I}$ phase transition does not occur in C(20):C(20:1Δ^{13})PC even at a very high ethanol concentration of 100 mg/ml (Fig. 4).

Two distinct effects of ethanol on the phase transition behavior and the phase structure of the lipid bilayer composed of monounsaturated PC have been observed as just discussed above. Moreover, these two effects can be definitely attributed to the different positions of the single Δ-bond in the *sn*-2 acyl chain of the lipid molecule. Hence, we need to examine some representative structures of C(20):C(20: 1Δ^n)PC packed in the gel-state bilayer for an understanding of the origin of the two distinct ethanol effects. Recently, a simple molecular model for the monounsaturated phospholipids packed in the gel-state bilayer has been advanced, and this model can explain adequately the experimental observations of various chain-melting characteristics exhibited by monounsaturated PC or PE [11,13]. Three interesting aspects of this model are worth mentioning. (1) The monounsaturated *sn*-2 acyl chain in the gel-state bilayer is assumed to adopt a crankshaft-like motif, consisting of two unequal chain segments linked by a Δ-containing kink sequence. (2) The long linear segment is assumed to adopt an all-*trans* conformation; hence, it can undergo intramolecularly and intermolecularly van der Waals attractive interactions with its neighboring all-*trans* acyl chains. (3) The short chain segment is assumed to be disordered at $T<T_m$, thus containing both *trans* and *gauche* rotamers in the gel-state bilayer.

With this simple molecular model in mind, the energy-minimized structures of C(20):C(20:1Δ^8)PC and C(20):C(20:1Δ^{13})PC are constructed by molecular mechanics simulations [2], and the molecular graphics representations of these two energy-minimized structures are illustrated in Fig. 5. It should be mentioned, however, that the molecular structures shown in Fig. 5 are energy-minimized conformations of lipids packed in the crystalline state. Most importantly, the conformations of these two positional isomers are different. Specifically, the short chain segment of the kinked *sn*-2 acyl chain of C(20):C(20:1Δ^8)PC is positioned in the upper chain region near the H_2O/hydrocarbon interface, while the short chain segment of C(20):C(20:1Δ^{13})PC is in the lower chain region away from the H_2O/hydrocarbon interface. These different conformations persist when these two positional isomers, C(20):C(20:1Δ^8)PC and C(20):C(20:1Δ^{13})PC, are packed in the gel-state bilayer. However, in the gel-phase bilayer the short segments in the *sn*-2 acyl chains of the two positional isomers are not all-*trans* as illustrated in Fig. 5; instead, they are rotationally disordered containing both *trans* and *gauche* rotamers.

Next, let us consider the structural as well as the energetic difference between the normal $L_{\beta'}$ gel-phase bilayer and the fully interdigitated $L_{\beta I}$ gel-phase bilayer. In the $L_{\beta'}$ gel-phase, the *sn*-1 acyl chain of one PC molecule is juxtaposed to the *sn*-2 acyl chain of another PC molecule from the opposing leaflet. Hence, the chain terminal methyl groups of each PC molecule are buried in the hydrocarbon core of the lipid bilayer. In the fully interdigitated $L_{\beta I}$ gel-phase, both the *sn*-1 and the *sn*-2 acyl chains of a PC molecule extend across the length of the whole hydrocarbon core, with their chain methyl termini facing the aqueous medium. In this packing mode, the exposure of methyl ends to the water is energetically unfavorable, and the unfavorable interaction is proportional to the product of the surface tension and the exposed surface area of the two acyl chain ($\gamma\cdot 2A$) [14]. In the presence of ethanol, this unfavorable energy is reduced somewhat due to the decrease in the surface tension and the shielding of the methyl end of each acyl chain by the ethyl moiety of ethanol. In the absence of ethanol, the magnitude of the unfavorable interaction can also vary, depending on the water accessible surface area of the chain end. If

the effective surface area is rather large, it is possible that the $L_{\beta I}$ phase is energetically so unfavorable that the ethanol-induced $L_{\beta'} \rightarrow L_{\beta I}$ transition will not occur. The highly asymmetric C(12):C(20)PC, for example, does not undergo the ethanol-induced $L_{\beta'} \rightarrow L_{\beta I}$ transition [2,4]. This can be attributed to the large surface area of the *sn*-2 acyl chain in C(12):C(20)PC that, due to the high asymmetry of the two acyl chains, would be accessible to water in the $L_{\beta I}$ phase.

As shown in Fig. 5, the short segment of the *sn*-2 acyl chain of C(20):C(20:1Δ^{13})PC is in the lower chain region. The chain terminus of this short segment would be exposed to the aqueous medium, if C(20):C(20:1Δ^{13})PC molecules were packed in the fully interdigitated $L_{\beta I}$ phase. According to the third basic feature of the molecular model of monounsaturated lipid discussed earlier, this short segment is, at $T < T_m$, rotationally disordered, consisting of *trans* and *gauche* rotamers. Although the precise structural details of this disordering state are not known, the effective cross-sectional area of this dynamic short segment near the chain end appears to increase by at least 1.7-fold over the actual cross-sectional area of an all-*trans* chain terminal [15]. This increase in the effective cross-sectional area of the short segment at $T < T_m$ means that the unfavorable interaction (γ2A) between the chain termini of C(20):C(20:1Δ^{13})PC and the aqueous medium must increase appreciably. As a result, the free energy of the C(20):C(20:1Δ^{13})PC bilayer in the fully interdigitated gel state ($L_{\beta I}$) can be assumed to be considerably larger than that of the C(20):C(20:1Δ^{13})PC bilayer packed in the non-interdigitated $L_{\beta'}$ gel-phase. This large free energy difference suggests a molecular interpretation as to why ethanol at the concentration up to about 100 mg/ml is unable to induce the $L_{\beta'} \rightarrow L_{\beta I}$ phase transition for the C(20):C(20:1Δ^{13})PC bilayer. Similarly, the large unfavorable interaction between the chain termini of C(20):C(20:1Δ^{13})PC and the aqueous medium also forms a plausible basis for interpreting the non-biphasic effect of ethanol on the T_m of C(20):C(20:1Δ^{13})PC as observed in the plot of T_m versus [EtOH] shown in Fig. 2. Likewise, the same interpretation can also be applied to the non-biphasic effect of ethanol on the normalized T_m of C(20):C(20:1Δ^{11})PC and C(20):C(20:1Δ^{17})PC as observed in Fig. 3. For C(20):C(20:1Δ^{11})PC and C(20):C(20:1Δ^{17})PC, the dynamically disordered short segment is also positioned in the lower region of the *sn*-2 hydrocarbon chain, which may give rise to a large unfavorable interaction with water.

A closer inspection of Fig. 3 reveals that, for lipids with a lower disordered short segment in the *sn*-2 acyl chain, the magnitude of the $|\Delta T_m|$ value at a given [EtOH] has the following decreasing order: C(20):C(20:1Δ^{17})PC > C(20):C(20:1Δ^{13})PC > C(20):C(20:1Δ^{11})PC. It has been suggested that the ethanol-induced T_m depression can be treated thermodynamically as the freezing point depression [3]. Hence, the depression of the T_m (or $|\Delta T_m|$) is related to the square of the phase transition temperature in the absence of ethanol (T_m^2); in addition, the depression of the T_m is also inversely related to the transition enthalpy [1]. The transition enthalpy is rather insensitive to the position of the Δ-bond for these positional isomers [11]. In contrast, the T_m depends strongly on the position of the Δ-bond in the *sn*-2 acyl chain. Specifically, the T_m values of lipid bilayers prepared individually from C(20):C(20:1Δ^{17})PC, C(20):C(20:1Δ^{13})PC and C(20):C(20:1Δ^{11})PC are 49.7, 22.1 and 19.4°C, respectively, as shown in the inset of Fig. 3. Based on these T_m values, the magnitude of the ethanol-induced T_m depression can be expected to be the largest for C(20):C(20:1Δ^{17})PC followed by C(20):C(20:1Δ^{13})PC and C(20):C(20:1Δ^{11})PC. This decreasing order is indeed observed in Fig. 3 for C(20):C(20:1Δ^{17})PC, C(20):C(20:1Δ^{13})PC and C(20):C(20:1Δ^{11})PC.

In the case of C(20):C(20:1Δ^{8})PC, the short segment of the kinked *sn*-2 acyl chain is located in the upper hydrocarbon region near the H_2O/hydrocarbon interface and the long segment of the kinked *sn*-2 acyl chain is in the lower hydrocarbon region (Fig. 5). When C(20):C(20:1Δ^{8})PC molecules are packed in the fully interdigitated $L_{\beta I}$ gel-phase bilayer, the methyl ends of the long all-*trans* (or fully extended) segment of the kinked *sn*-2 acyl chain and the all-*trans sn*-1 acyl chain of each PC molecule are in direct contact with water. This situation is analogous to saturated PC molecules packed in the $L_{\beta I}$ gel-phase, in which the tails of two fully extended acyl chains of each lipid molecule are facing the aqueous medium. Most importantly, the effective

cross-sectional area of the acyl chain is at the minimum as the chain adopts an all-*trans* conformation. Hence, the water accessible surface area of the tail group (A) is also at minimal, leading to a minimal strength of the unfavorable interaction, γ·2A. Under the condition of fully extended all-*trans* conformation of the chain terminal, the free energy of the $L_{\beta I}$ gel-phase is still higher than that of the $L_{\beta'}$ gel-phase. However, as demonstrated by most saturated PC, the free energy difference between the $L_{\beta I}$ and the $L_{\beta'}$ gel-states can be overcome by the addition of a high concentration of ethanol into the aqueous medium [4]. The observed biphasic effect of ethanol on the T_m of C(20):C(20:1Δ^8)PC shown in Fig. 1 can thus be explained as being most likely due to the all-*trans* conformation of the long segment of the *sn*-2 acyl chain, with which the tail surface area accessible to H_2O is minimal. It should be noted, however, that in comparison with saturated C(20):C(19)PC the inflection point of the biphasic curve for C(20):C(20:1Δ^8)PC occurs at a higher concentration of ethanol (Fig. 1). The physical basis underlying this larger $[EtOH]_{TC}$ value is not fully understood. Nevertheless, it does imply that the free energy difference between the $L_{\beta I}$ and the $L_{\beta'}$ gel-states for C(20):C(20:1Δ^8)PC is larger than that for saturated C(20):C(19)PC.

It should also be mentioned that C(20):C(20:1Δ^5)PC exhibits a ΔT_m profile with a positive slope when the ΔT_m value is plotted against [EtOH] as shown in Fig. 3. Moreover, X-ray diffraction results indicate that at room temperatures the C(20):C(20:1Δ^5)PC bilayer adopts the fully interdigitated $L_{\beta I}$ motif under the condition of $[EtOH] \geq 20$ mg/ml. Like C(20):C(20:1Δ^8)PC, the short and long segments of the kinked *sn*-2 acyl chain of C(20):C(20:1Δ^5)PC are positioned in the upper and lower hydrocarbon regions, respectively. Hence, it is not unexpected that the C(20):C(20:1Δ^5)PC bilayer can undergo the ethanol-induced $L_{\beta'} \rightarrow L_{\beta I}$ phase transition. Interestingly, the observed $[EtOH]_{TC}$ value of $\sim$20 mg/ml for C(20):C(20:1Δ^5)PC is considerably lower than those obtained with C(20):C(20:1Δ^8)PC and C(20):C(19)PC. For C(20):C(20:1Δ^5)PC, a unique structural feature is the position of its Δ-bond, which is located very near ($\sim$3 Å) to the H_2O/hydrocarbon interface. In general, the Δ-bond in the *sn*-2 acyl chain can perturb locally the lateral chain–chain van der Waals attractive interaction in the gel-state bilayer. Moreover, as the Δ-bond is positioned at $\sim$3 Å away from the H_2O/hydrocarbon interface, H_2O molecules can diffuse readily into this perturbed local region and orient themselves in the immediate vicinity of the Δ^5-bond. These penetrated H_2O molecules have decreased entropy because of their reduced mobility as constrained by the hydrophobic chains. In addition, these highly ordered water molecules could further weaken locally the lateral chain–chain interaction. Consequently, in the $L_{\beta'}$ phase C(20):C(20:1Δ^5)PC differs from C(20):C(19)PC and C(20):C(20:1Δ^8)PC in terms of the degree of hydration. As ethanol is added, the bound water in the immediate neighborhood of the Δ^5-bond in the gel-state bilayer will be displaced by ethanol. The released water molecules will gain freedom of motion, which, in turn, makes a favorable contribution to the ethanol-induced $L_{\beta'} \rightarrow L_{\beta I}$ phase transition. The relatively high degree of hydration of C(20):C(20:1Δ^5)PC in the $L_{\beta'}$ phase can, therefore, be considered as a plausible basis to explain why the C(20):C(20:1Δ^5)PC bilayer is prone to convert from the $L_{\beta'}$ gel-phase to the $L_{\beta I}$ gel-phase in the presence of ethanol.

In recent years, it has been shown by many biophysical studies that a high concentration of ethanol can induce the lipid bilayer to undergo an isothermal phase transition, at $T < T_m$, from the normal $L_{\beta'}$ phase to the fully interdigitated $L_{\beta I}$ phase. All these studies, however, were confined to phospholipids with *sn*-1 saturated/*sn*-2 saturated acyl chains. In this communication, we have studied the effect of ethanol on the phase transition behavior and the phase structure of the lipid bilayer prepared from mixed-chain *sn*-1 saturated/*sn*-2 unsaturated PC such as C(20):C(20:1Δ^n)PC with $n = 5$, 8, 11, 13 and 17. Our DSC and X-ray diffraction results show for the first time that lipid bilayers composed of mixed-chain C(20):C(20:1Δ^n)PC with $n = 5$ and 8 can indeed undergo the ethanol-induced isothermal $L_{\beta'} \rightarrow L_{\beta I}$ phase transition at $T < T_m$. Moreover, the concentration of ethanol required to induce such an isothermal phase transition can be rather low for mixed-chain C(20):C(20:1Δ^5)PC. It is worth mentioning that phospholipids isolated from animal cell membranes are predominantly mixed-chain *sn*-1 saturated/*sn*-2 unsaturated lipids. The phospholipids

employed in this communication are thus biologically relevant. However, the physiological consequences of the observed ethanol-induced isothermal $L_{\beta'} \rightarrow L_{\beta I}$ phase transition in animal cell membranes are not yet understood at the present time.

Acknowledgements

This work was supported, in part, by US Public Health Service Grants GM-17452 (C.-h.H.) and GM-27278 (T.J.M.) from NIGMS, National Institutes of Health, Department of Health and Human Services.

References

[1] E.S. Rowe, Effects of alcohol on membrane lipids, in: R. Watson (Ed.), Alcohol and Neurobiology, CRC Press, Boca Raton, FL, 1992, pp. 239–267.
[2] S. Li, H-n. Lin, G. Wang, C. Huang, Effects of alcohols on the phase transition temperatures of mixed-chain phosphatidylcholines, Biophys. J. 70 (1996) 2784–2794.
[3] S.A. Simon, T.J. McIntosh, Interdigitated hydrocarbon chain packing causes the biphasic transition behavior in lipid/alcohol suspensions, Biochim. Biophys. Acta 773 (1984) 169–172.
[4] C. Huang, T.J. McIntosh, Probing the ethanol-induced chain interdigitations in gel-state bilayers of mixed-chain phosphatidylcholines, Biophys. J. 72 (1997) 2702–2709.
[5] W.E.M. Lands, P. Hart, Control of fatty acid composition in glycerolipids, J. Am. Oil Chem. Soc. 43 (1966) 290–295.
[6] G. Wang, S. Li, H-n. Lin, E.E. Brumbaugh, C. Huang, Effects of various numbers and positions of *cis* double bonds in the *sn*-2 acyl chain of phosphatidylethanolamine on the chain-melting temperature, J. Biol. Chem. 274 (1999) 12289–12299.
[7] H-n. Lin, Z-q. Wang, C. Huang, Differential scanning calorimetry study of mixed-chain phosphatidylcholines with a common molecular weight identical with diheptadecanoyl phosphatidylcholine, Biochemistry 29 (1990) 7063–7072.
[8] T.J. McIntosh, Differences in hydrocarbon chain tilt between hydrated phosphatidylethanolamine and phosphatidylcholine bilayers. A molecular packing model, Biophys. J. 29 (1980) 237–246.
[9] T.J. McIntosh, S.A. Simon, The hydration force and bilayer deformation a reevaluation, Biochemistry 25 (1986) 4058–4066.
[10] T.J. McIntosh, R.V. McDaniel, S.A. Simon, Induction of an interdigitated gel phase in fully hydrated lecithin bilayers, Biochim. Biophys. Acta 731 (1983) 109–114.
[11] G. Wang, H-n. Lin, S. Li, C. Huang, Phosphatidylcholines with sn-1 saturated and *sn*-2 *cis*-monounsaturated acyl chains: their melting behavior and structures, J. Biol. Chem. 270 (1995) 22738–22746.
[12] W. Lesslauer, J.E. Cain, J.K. Blasie, X-ray diffraction studies of lecithin bimolecular leaflets with incorporated fluorescent probes, Proc. Natl. Acad. Sci. USA 69 (1972) 1499–1503.
[13] S. Li, G. Wang, H. Lin, C. Huang, Calorimetric studies of phosphatidylethanolamines with saturated *sn*-1 and dienoic *sn*-2 acyl chains, J. Biol. Chem. 273 (1998) 19009–19018.
[14] J.F. Nagle, Theory of main lipid bilayer phase transition, Annu. Rev. Phys. Chem. 31 (1980) 157–195.
[15] C. Huang, S. Li, Computational molecular models of lipid bilayers containing mixed-chain saturated and monounsaturated acyl chains, in: D.D. Lasic, Y. Barenholz (Eds.), Handbook of Nonmedical Applications of Liposomes, vol. I, CRC Press, Boca Raton, FL, 1996, pp. 173–194.